American Mineralogist, Volume 70, pages 1217–1223, 1985

Tourmaline solid solutions in the system $MgO–Al_2O_3–SiO_2–B_2O_3–H_2O$

PHILIP E. ROSENBERG AND FRANKLIN F. FOIT, JR.

Department of Geology
Washington State University
Pullman, Washington 99164

Abstract

A narrow range of tourmaline solid solutions has been synthesized in the system $MgO–Al_2O_3–SiO_2–B_2O_3–H_2O$ in the presence of excess silica, B_2O_3 and H_2O in the temperature range 400–800°C at a pressure of 1 kbar. Tourmalines were characterized by unit-cell dimensions and partial chemical (AEM) analyses, which were used to calculate approximate structural formulas. Mg/Al ratios in the 9b octahedral site are either ≥ 2 or < 1; alkali-site occupancy and ^{IV}Al decrease with increasing temperature and protons are generally deficient. Tourmalines closely approaching the ideal defect end-member, $\square(Mg_2Al)Al_6(BO_3)_3Si_6O_{18}(OH)_4$, were synthesized at high-temperatures.

When talc or mullite is also present, the substitution $Si^{4+} + Mg^{2+} = 2Al^{3+}$ predominates in the forward or reverse direction resulting in partial solid solution toward talc or mullite, respectively. The substitution $2H^+ + \square = Mg^{2+}$ exchanges protons for small amounts of Mg^{2+} which enters the alkali-site in the presence of excess talc. Inferred subsolidus phase areas projected into the system $MgO–Al_2O_3–SiO_2$ include two three-phase areas (tourmaline solid solution, quartz and talc or mullite), and one two-phase area (tourmaline solid solutions and quartz).

Alkaki-free tourmalines have a *P–T* stability range comparable to that of alkali-bearing tourmalines and, therefore, probably exist in nature.

Introduction

Although tourmalines approaching the alkaki-free end-member have recently been reported in nature (Towatana, 1985) most natural tourmalines do not closely approach this composition. Many tourmalines are, however, somewhat alkali-deficient (Foit and Rosenberg, 1977) and, thus, alkali-free tourmalines are important end-members of the tourmaline group. Yet, despite recent investigations (Rosenberg and Foit, 1979; Werding and Schreyer, 1984), little is known of the substitutional chemistry of these tourmalines.

A decade ago alkali-free tourmalines were synthesized in the system $MgO–Al_2O_3–SiO_2–B_2O_3–H_2O$ between 400 and 750°C at 1 kbar (Rosenberg and Foit, 1975). Later, two larger samples were prepared at 450 and 600°C from a single starting composition in order to obtain enough material for complete characterization (Rosenberg and Foit; 1977, 1979). Because alkali-free tourmaline was thought to be related to dravite, $NaMg_3Al_6(BO_3)_3Si_6O_{18}(OH)_4$, by the substitution $Al^{3+} + \square = Mg^{2+} + Na^+$, a crystalline phase corresponding to the structural formula $\square(Mg_2Al)Al_6(BO_3)_3Si_6O_{18}(OH)_4$ was anticipated. However, the tourmalines synthesized proved to be poorer in silica and richer in alumina and magnesia than this ideal defect composition. Although only quartz and H_3BO_3 were observed to coexist with the two alkali-free tourmalines characterized in the previous study, recent microscopic examination of the products of several of the preliminary experiments revealed the presence of small amounts of talc in addition to quartz and H_3BO_3.

An investigation of alkali-free tourmalines in assemblages with talc in the system $MgO–Al_2O_3–SiO_2–B_2O_3–H_2O$ was undertaken in order to compare the compositions and unit-cell dimensions of alkali-free tourmalines in the presence and absence of talc. Compositional differences were expected because substitutions of the type $Mg^{2+} + H^+ = Al^{3+}$ could lead to tourmaline compositions richer in Mg than those previously reported (Rosenberg and Foit, 1979). The recent claim of Werding and Schreyer (1984) that the only tourmaline composition in the system $MgO–Al_2O_3–SiO_2–B_2O_3–H_2O$ over a wide range of temperatures, pressures and starting compositions corresponds to the ideal defect end-member $\square(Mg_2Al)Al_6(BO_3)_3Si_6O_{18}(OH)_4$ emphasized the need for further studies in the system.

Synthesis

Mechanical mixtures were prepared from reagent-grade MgO, γ-Al_2O_3 (synthesized at 700°C for 1½ hours from $AlCl_3 \cdot 6H_2O$), quartz (Minas Gerais, Brazil) and B_2O_3 (spec-pure) in excess of the stoichiometric amount required to form tourmaline as in the previous study (Rosenberg and Foit, 1979). Experimental results reported here were obtained using three starting compositions; A, B, C (Table 1). Starting composition A is the mechanical mixture used by Rosenberg and Foit (1979).

Tourmaline-bearing assemblages were synthesized from these starting compositions in the temperature range 400–800°C at 1

0003–004X/85/1112–1217$02.00

Table 1. Starting compositions (mole %)

	A	B	C
SiO_2	41.8	46.7	38.16
Al_2O_3	24.3	9.7	34.24
MgO	13.9	25.5	7.6
B_2O_3	20.0	18.1	20.0

kbar in sealed gold tubes containing excess water (solid/water ratio ~2/1). In general, the duration of experiments was doubled until no further change in the nature or approximate proportions of the phases present was observed for a particular temperature (except at 500° and 800°C) and bulk composition. Solid phases were identified by X-ray diffractometry and by optical and, in several cases, electron microscopy. Experimental results are given in Table 2; data for samples 267 and 251 were reported previously (Rosenberg and Foit, 1979).

Characterization

Synthetic alkali-free tourmalines were too small to permit measurement of optical properties and, therefore, they were characterized by their unit-cell dimensions and chemical compositions (Table 3).

The unit-cell dimensions of alkali-free tourmalines were refined in space group *R3m* by least squares methods using the seven measurable X-ray reflections (internally calibrated using NaCl as a standard) observed for each sample. Two distinct groups are apparent (Fig. 1) each of which includes one of the two samples reported previously (267, 251; Table 3). Since the unit-cell dimensions of tourmaline depend, to a first approximation, on the contents of the octahedral sites (Rosenberg and Foit, 1979; Ozaki, 1982), these two groups are thought to represent distinct octahedral site occupancies. The cell dimensions of the group which approximate those of elbaite (Fig. 1), imply a Mg/Al ratio of about unity in the larger 9b octahedral site while the larger cell dimensions of the other group imply a Mg/Al ratio of approximately two in this site based on an interpolation between dravite and elbaite (Rosenberg and Foit, 1979). The spread in *a* values within the group representing larger cell dimensions may be due to disordering of Mg and Al within and/or between the 9b and 18c octahedral sites (Werding and Schreyer, 1984), which tends to increase at higher temperatures. All of the tourmalines synthesized at high temperatures (≥700°C) in this study and by Werding and Schreyer (Fig. 1) have *a* dimensions greater than 15.89Å while all tourmalines synthesized at lower temperatures (400–600°C) have smaller *a* dimensions.

Table 2. Experimental results

Temp.(°C)	Run No.	Starting Composition[2]	Duration (days)	Products[3]
800	179	B	9	Ta; Tm (Qtz)
750	236	A	34	Tm; (Qtz)
700	207	A	67	Tm; (Qtz)
	208	B	67	Ta; Tm
600	187	B	89	Ta; Tm
	267	A	70	Tm; Qtz
	273	C	119	Tm
500	197	A	49	Tm; (Qtz)
450	251	A	70	Tm; Qtz
	255	A	84	Tm; Qtz; (Ta)
400	243	A	95	Tm; Qtz; (Ta)

1) A summary of critical data representing over 300 experiments.
2) A, B, C see Table 1; excess H_2O added to all experiments.
3) Ta, talc; Tm, tourmaline; Qtz, quartz. H_3BO_3 and aqueous fluid present in all experiments. Bracketed phases present in minor amounts, detected by optical and/or electron microscopy.

Electron microprobe analysis of alkali-free tourmaline was not feasible due to the small size of the synthetic crystals. Partial chemical analyses were obtained by means of analytical electron microscopy (AEM) using the procedures described by Rosenberg and Foit (1979). Ten or more random point analyses of tourmaline and eight of talc crystals were averaged to obtain count-rate data for MgO, Al_2O_3 and SiO_2. Relative percentages of these oxides were then calculated using natural dravite (Dobruwa Carinthia, Austria, NMNH 103791; Swanson et al., 1964) as a standard and assuming direct proportionality of the ratio, percent oxide/average counts per unit time, between sample and standard. Because crystal thickness (absorption) cannot be measured under the AEM only relative oxide percentages could be obtained.

Counting statistics in AEM analysis have been discussed by Champness et al. (1982). Assuming Gaussian behavior, at the 2σ confidence level, the relative error in the number of counts, I, is $2\sqrt{I}$. On this basis for the ten or more random point analyses reported for each tourmaline sample the relative error is less than 1% for SiO_2 and Al_2O_3 and 1–3% for MgO. Thus, the precision of AEM analyses is probably similar to that achieved using other instrumental methods.

Partial chemical analyses (Table 3) are reported for ten synthetic tourmalines and for two synthetic talcs (208, 243) containing appreciable Al; talcs in samples 179 and 187 are much closer to end-member composition based on an analytical survey of several crystals in each sample.

As reported in the previous investigation (Rosenberg and Foit, 1979) alkali-free tourmalines synthesized from starting composition A are poorer in SiO_2 and richer in Al_2O_3 and MgO than the starting material; small amounts of quartz are present in these samples. Furthermore, tourmaline compositions in experiments at and above 600°C are approximately 5 mole percent higher in SiO_2 than those in experiments at 400° and 450°C. Projections of these tourmaline compositions into the system MgO–Al_2O_3–SiO_2 lie close to an extension of the line drawn between starting composition A and SiO_2 (Fig. 2; Rosenberg and Foit, 1979). Although no talc was observed in sample 251, small amounts were identified in sample 255 which was synthesized from the same starting composition in a somewhat longer experiment at the same temperature and produced tourmaline of nearly identical composition (Tables 2 and 3; Fig. 2). Thus, a trace of talc may be present in sample 251.

Table 3. Partial chemical analyses and unit-cell dimensions

Run No.:	179	236	207	208	187	267	273	197	251	255	243
	Tourmaline										
SiO_2	50.55	50.30	49.98	49.05	49.24	49.18	50.50	n.d.[3]	44.21	44.56	44.55
Al_2O_3	30.15	31.60	31.33	29.54	29.92	32.80	36.34	n.d.	34.86	34.69	35.88
MgO	19.30	18.10	18.70	21.41	20.84	18.02	13.16	n.d.	20.94	20.75	19.57
a (Å)	15.894(3)	15.906(3)	15.905(3)	15.912(10)	15.882(6)	15.884(2)	15.842(5)	15.879(8)	15.849(5)	15.840(3)	15.839(3)
c (Å)	7.126(2)	7.119(2)	7.127(2)	7.124(7)	7.126(4)	7.128(1)	7.100(4)	7.128(6)	7.108(3)	7.111(2)	7.103(2)
	Talc										
SiO_2				56.89							56.23
Al_2O_3				3.23							3.61
MgO				39.89							40.17

1) Partial compositions recalculated to 100 mole percent.
2) Refined from measurements of seven X-ray reflections/sample.
3) n.d. not determined

Assemblages synthesized from starting composition B contain large proportions of both tourmaline and talc (Table 2). These tourmalines have higher MgO/Al_2O_3 ratios and, therefore, lie closer in composition to talc than do those synthesized between 600° and 800°C from starting composition A (Table 3). The extent of solid solution toward talc from tourmaline, synthesized at comparable temperatures from starting composition A, is about 7.5%.

Starting composition C is represented by a single experiment (273, Table 2) of long duration at 600°C. Although tourmaline is the only phase other than H_3BO_3 conclusively identified in this sample, a single unassigned

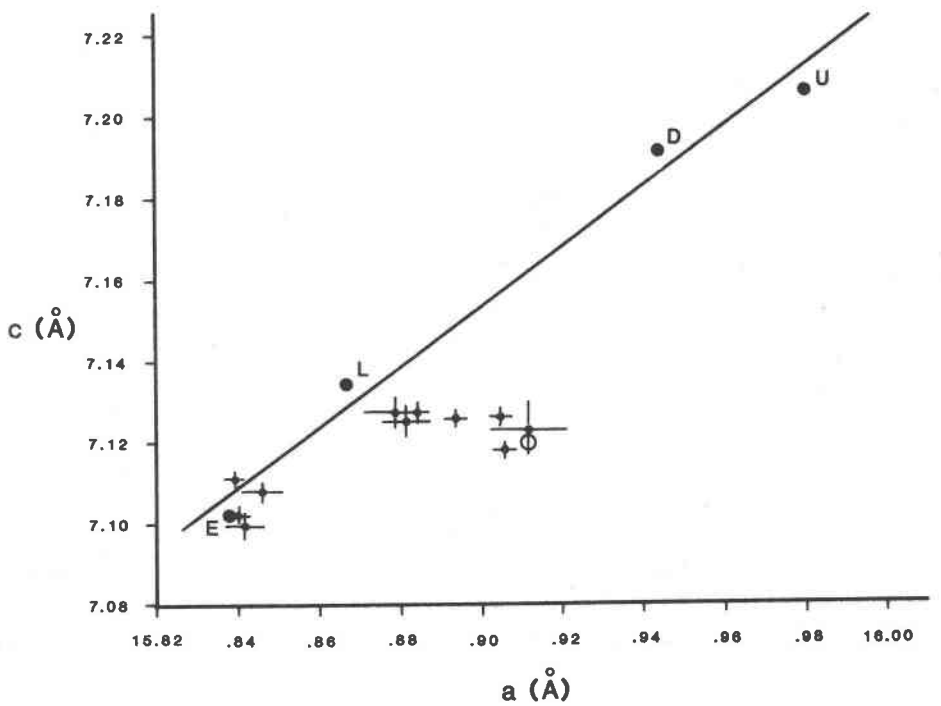

Fig. 1. Diagram showing the relationship between the unit-cell dimensions of synthetic alkali-free tourmalines (solid dots and 1σ error bars, this study; open circle, Werding and Schreyer, 1984) and those of dravite, D (Hirose Mine, Tottori Prefecture, Japan; Kitahara, 1966); elbaite, E (San Diego Co., Calif.; Donnay and Barton, 1972); liddicoatite, L (Dunn et al., 1977a) uvite, U (Dunn et al., 1977b), and schorl, S (Donnay and Barton, 1972).

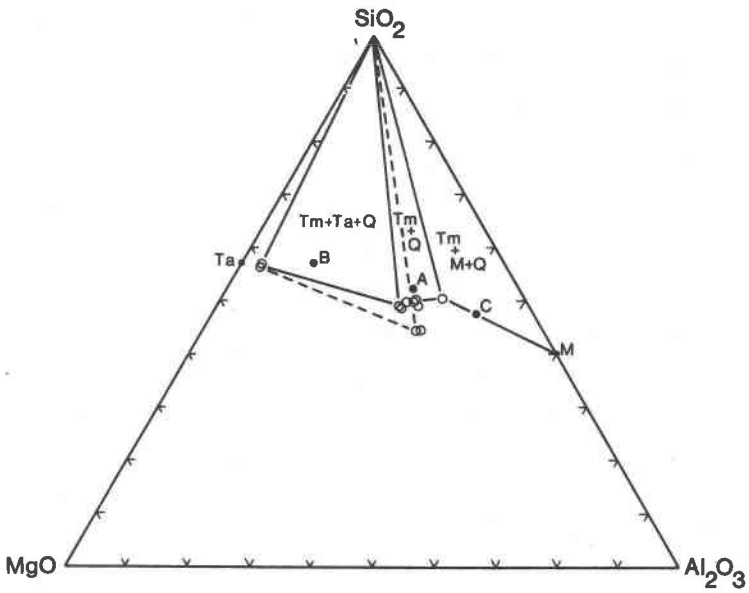

Fig. 2. Ternary diagram showing compositions (mole percent) of the starting mixtures A, B and C, alkali-free tourmalines and inferred compatibility triangles projected into the system $MgO–Al_2O_3–SiO_2$. Solid lines, 600–800°C; dashed lines, 400–500°C; Tm, tourmaline; Ta, talc; Q, quartz; M, mullite.

X-ray reflection is consistent with the presence of mullite, presumably B-bearing. Tourmaline 273 lies close to a line connecting starting composition A with mullite (Fig. 2) suggesting that solid solution extends about 25% from ideal defect tourmaline toward mullite.

Compatibility triangles for the assemblages tourmaline + quartz ± talc + B_2O_3(l) + aqueous fluid can be constructed for two temperature ranges, 600–800°C (solid lines, Fig. 2) and 400–450°C (dashed lines) based on the analytical data in Table 3. Although talc compositions in samples

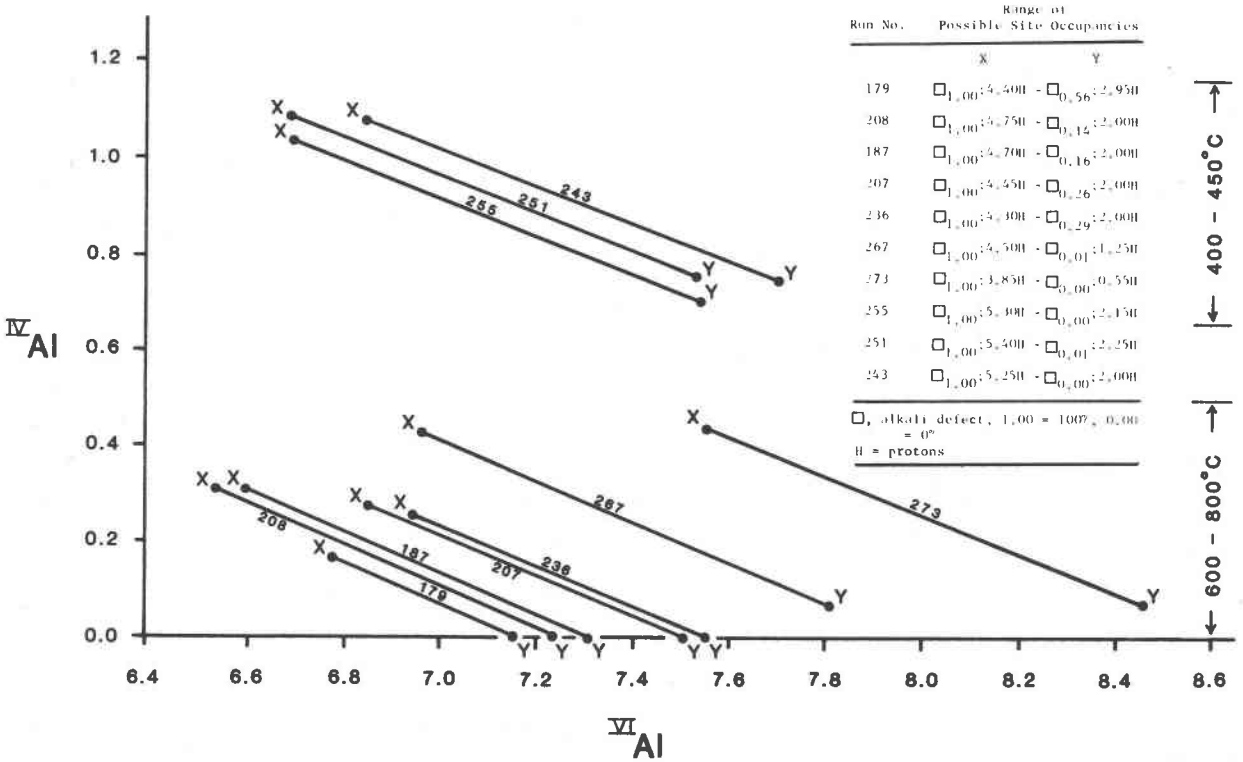

Fig. 3. Diagram showing the range of probable site occupancies in alkali-free tourmalines: ^{VI}Al, aluminum in octahedral coordination; ^{IV}Al, aluminum in tetrahedral coordination. X and Y correspond to extremes in site occupancies for each tourmaline composition (See Table 4).

208 and 243 have been used in the construction of compatibility triangles, the stability of these Al-bearing talc solid solutions is uncertain. Stable talc solid solutions may lie closer to the talc end-member as suggested by an analytical survey (AEM) of talc crystals in samples 187 and 179. The position of the tourmaline-talc tie-lines and the presence of trace amounts of quartz in sample 179 (Fig. 2) indicate that small amounts of excess silica are probably present in all assemblages synthesized from starting composition B. Assuming the presence of mullite in sample 273, a tentative tourmaline–mullite tie-line can also be constructed. Note that composition C lies on the line between tourmaline 273 and boron-free mullite (Fig. 2). Thus two, three-phase areas (tourmaline, talc, quartz, and tourmaline, mullite, quartz) and one, two-phase (tourmaline, quartz) area may be inferred, with solid solution extending from tourmaline 208 to 273 at 600°C (Table 3).

By assuming that boron is present in stoichiometric quantities and that the number of protons is variable as in natural tourmaline (Fortier and Donnay, 1975; Foit and Rosenberg, 1977), a series of structural formulas can be calculated for each alkali-free tourmaline based on 31 (O, OH) following procedures commonly used in tourmaline structural studies (Rosenberg and Foit, 1979). Briefly, the sequence is: (1) Al^{3+} supplements Si^{4+} to fill the tetrahedral site; (2) remaining Al^{3+} preferentially fills the smaller octahedral site (18c); excess Al^{3+} occupies the larger octahedral site (9b) which is then filled by Mg^{2+}; (3) excess Mg^{2+} enters the alkali-site; alkali-site vacancies are possible; (4) formulas with excess cations or octahedral vacancies are unlikely.

Numbers of protons producing possible structural formulas, as defined by the above assumptions, vary from 1.25 to 5.4. The corresponding range of site occupancies for each alkali-free tourmaline is shown in Figure 3. Assuming that boron is present in stoichiometric quantities, variables in the structural chemistry are numbers of (1) protons, (2) alkali-site vacancies, (3) $^{IV}Al^{3+}$, and (4) $^{VI}Al^{3+}$. The structural formulas are univariant in that if one of these variables were known then the others would be fixed and a unique structural formula could then be specified for each alkali-free tourmaline. However, even without knowledge of these variables, the chemical data serve to constrain site occupancies within broad limits (Fig. 3).

Discussion

Inferred structural formulas

Site occupancies in alkali-free tourmalines cannot be specified using AEM data alone. However, an estimate of any one of the four above mentioned, structural-chemical variables would define values for the others and, thus, provide an approximate structural formula.

Estimation of octahedral site occupancies of alkali-free tourmalines is possible through a knowledge of their cell parameters. An approximate linear relationship between unit-cell dimensions and octahedral site occupancies, which has been shown to exist for natural dravites and elbaites, has been used to estimate site occupancies in alkali-free tourmalines (Rosenberg and Foit, 1979). The unit-cell dimensions of schorls follow a linear trend different from that of dravites (e.g. Werding and Schreyer, 1984) probably because Fe^{2+}, a Jahn-Teller ion, prefers distorted octahedral sites (Walsh et al., 1974).

Distortion of the schorl 9b octahedral site is about the same as it is for aluminous dravite whereas this structural site is less distorted in dravite (Fig. 3; Foit and Rosenberg, 1979). The alkali-free, aluminous dravites synthesized by Werding and Schreyer (1984) lie close to the elbaite schorl trend (Fig. 1) suggesting that octahedral distortion in these tourmalines is more similar to that in schorl than to dravite.

Accepting, in principle, the linear dependence of the unit-cell dimensions of natural tourmalines on their Mg(Li)/Al ratios (Rosenberg and Foit, 1979), the approximate number of Al atoms in octahedral coordination has been estimated and used to fix the other structural-chemical variables. A linear relationship between the unit-cell dimensions of elbaite, liddicoatite, dravite and uvite (Fig. 1) has been defined by regression analysis of the cell parameters of four natural tourmalines closely approaching these endmember compositions. A second line connects the unit-cell dimensions of natural schorl with those of elbaite. Assuming that the divergence in a dimensions observed for the group of tourmalines with larger cell parameters, reflects varying distortion of the 9b site, two subgroups may be recognized, those with $a < 15.89$Å which lie close to the elbaite-dravite trend synthesized at and below 600°C and those with $a >$ 15.89Å which approach the elbaite-schorl trend synthesized at and above 700°C (Fig. 1). The greater disorder inferred in the schorl-like, aluminous dravites is consistent with their synthesis at higher temperatures.

The number of ^{VI}Al atoms in the structural formula of each alkali-free tourmaline was estimated by interpolation through a knowledge of the octahedral occupancies of the natural tourmalines. Perpendiculars were raised from the data points to the appropriate line (Fig. 1) in order to carry out this interpolation. Tourmalines with $a < 15.89$Å were referred to the elbaite-dravite trend while those with $a >$ 15.90Å were based on the elbaite-schorl relationship. Because tourmaline 179 lies midway in the range of a values ($a = 15.894$Å, Table 3), an average based on interpolations to both linear trends was used to estimate the number of ^{VI}Al atoms in this sample. The number of ^{VI}Al atoms for each synthetic tourmaline was then used to estimate the other structural-chemical variables by means of the univariant relationships shown in Figure 3. The resulting approximate structural formulas[1] (Table 4) are adequate for comparison and discussion. As in the study by Rosenberg and Foit (1979) synthesis of the anticipated ideal defect tourmaline, $\square(Mg_2Al)Al_6(BO_3)_3Si_6O_{18}(OH)_4$, in the system MgO–Al_2O_3–SiO_2–B_2O_3–H_2O was not accomplished. Several generalizations regarding synthetic alkali-

[1] The structural formula of tourmaline 197 has not been calculated because of the lack of analytical data but the Mg/Al ratio in octahedral coordination can be inferred from its unit-cell dimensions (Table 3; Fig. 1).

Table 4. Approximate structural formulas of alkali-free tourmalines

Run No.	Temp. (°C)	Approximate Structural Formula
179	800	$\square_{0.7}Mg_{0.3}(Mg_{2.0}Al_{1.0})Al_6(Si_{5.9}Al_{0.1})(BO_3)_3O_{18.5}(OH)_{3.5}$
236	750	$\square_{0.9}Mg_{0.1}(Mg_{2.0}Al_{1.0})Al_6(Si_{5.8}Al_{0.2})(BO_3)_3O_{17.9}(OH)_{4.1}$
207	700	$\square_{0.8}Mg_{0.2}(Mg_{2.0}Al_{1.0})Al_6(Si_{5.8}Al_{0.2})(BO_3)_3O_{18.1}(OH)_{3.9}$
208	700	$\square_{0.5}Mg_{0.5}(Mg_{2.1}Al_{0.9})Al_6(Si_{5.9}Al_{0.1})(BO_3)_3O_{18.9}(OH)_{3.1}$
187	600	$\square_{0.5}Mg_{0.5}(Mg_{2.0}Al_{1.0})Al_6(Si_{5.9}Al_{0.1})(BO_3)_3O_{19.0}(OH)_{3.0}$
267	600	$\square_{0.9}Mg_{0.1}(Mg_{2.0}Al_{1.0})Al_6(Si_{5.6}Al_{0.4})(BO_3)_3O_{17.7}(OH)_{4.3}$
273	600	$\square_{1.0}(Mg_{1.4}Al_{1.6})Al_6(Si_{5.6}Al_{0.4})(BO_3)_3O_{18.3}(OH)_{3.7}$
251	450	$\square_{0.1}Mg_{0.9}(Mg_{1.5}Al_{1.5})Al_6(Si_{5.2}Al_{0.8})(BO_3)_3O_{19.5}(OH)_{2.5}$
255	450	$Mg_{1.0}(Mg_{1.5}Al_{1.5})Al_6(Si_{5.3}Al_{0.7})(BO_3)_3O_{19.9}(OH)_{2.1}$
243	400	$\square_{0.1}Mg_{0.9}(Mg_{1.4}Al_{1.6})Al_6(Si_{5.2}Al_{0.8})(BO_3)_3O_{19.6}(OH)_{2.4}$
ideal		$\square_{1.0}(Mg_2Al)Al_6(Si_6)(BO_3)_3O_{18}(OH)_4$

free tourmaline are apparent:

(1) The alkali site is vacant or nearly so in all assemblages not in apparent equilibrium with talc regardless of temperature.

(2) In assemblages with talc alkali site occupancy tends to decrease from 90% at 400–450°C to 30% at 800°C. Since the effective size of any coordination polyhedron increases with increasing temperature, the alkali site probably becomes smaller with decreasing temperature and able to accommodate substantial Mg^{2+} below 500°C.

(3) Octahedral site occupancies are bimodally distributed; Mg/Al ratios in the 9b site are either ≥ 2 or ≤ 1; none are intermediate.

(4) ^{IV}Al tends to increase with decreasing temperature below 700°C in all assemblages.

(5) Protons are generally deficient (i.e., $H^+ < 4$) especially at 400–450°C but two tourmalines (236 and 267) have small proton excesses which may be accommodated in the alkali site as H_3O^+ or other positive-charge deficient sites.

Tourmaline solid solutions

At temperatures above 500°C, solid solution toward talc in talc-bearing assemblages takes place to a limited extent according to the equation $Si^{4+} + Mg^{2+} = 2Al^{3+}$. The substitution $2H^+ + \square = Mg^{2+}$ exchanges protons for a small amount of Mg^{2+} which enters the alkali-site but the amount of Mg^{2+} in the alkali site diminishes with increasing temperature, again demonstrating that occupation of the alkali-site by Mg^{2+} is not favored at high temperatures. At temperatures below 500°C there is little or no solid solution toward talc.

Solid solution toward mullite (tourmaline 273) takes place according to the reverse of the reaction for solid solution toward talc (i.e., $2Al^{3+} = Si^{4+} + Mg^{2+}$) with little or no contribution from the other substitutions. Excess Al^{3+} enters the 9b octahedral site (decreasing the Mg/Al ratio) and to a lesser extent the tetrahedral site.

Relation to other studies

Werding and Schreyer (1984) report the synthesis of a single tourmaline composition, corresponding to the ideal defect end-member, $\square(Mg_2Al)Al_6(BO_3)_3Si_6O_{18}(OH)_4$, in the system $MgO–Al_2O_3–SiO_2–B_2O_3–H_2O$ at temperatures between 300° and 870°C and pressures of 1–20 kbar. Their "invariant composition" is based on bulk chemical analyses but aside from water-content, they report an analysis for only one element in hand-picked tourmaline from a single experiment at 870°C and 20 kbar. While this analysis may be accurate, it does not seem adequate to represent tourmaline compositions over the entire *P–T–X* range of their experiments. However, the structural formula derived from these limited data is consistent with the results obtained in the present investigation. Since alkali-site vacancies increase and ^{IV}Al decreases with increasing temperature (Table 4), extrapolation to 870°C might well yield the ideal defect composition reported by Werding and Schreyer (1984). Furthermore, because Al^{3+} is significantly larger than Si^{4+}, experiments at 20 kbar (Werding and Schreyer, 1984) would certainly favor less substitution of Al in the tetrahedral sites than in experiments at 1 kbar (present investigation). Thus, the ideal defect end-member is thought to exist only at high pressures and/or temperatures.

In lieu of chemical analyses for their other samples Werding and Schreyer (1984) rely on a comparison of unit-cell dimensions to infer chemical compositions of tourmaline. Since their cell parameters form a tight cluster on an *a* vs. *c* diagram, they assume that all of their tourmalines have the same chemical composition, which may not be true. Tourmalines 243 and 273 (Table 3), for example, have very similar unit-cell dimensions but significantly different chemical compositions; 267 and 187 (Table 3) also illustrate this point. However, similar unit-cell dimensions do imply similar octahedral occupancies (Rosenberg and Foit, 1979).

It is interesting to note that the lattice parameters reported by Werding and Schreyer (1984) are similar to those obtained in this study for the group having larger cell dimensions which were synthesized at and above 600°C. It seems likely that, in the absence of talc, these tourmalines are all of very similar composition differing only in the degree of octahedral disorder.

Summary and conclusions

The existence of a narrow range of tourmaline solid solutions in the system $MgO–Al_2O_3–SiO_2–B_2O_3–H_2O$ has been demonstrated and the principal substitutions in the presence of excess silica, B_2O_3 and H_2O have been identified in the temperature range 400–800°C at a pressure of 1 kbar. Synthetic tourmalines were characterized by their unit-cell dimensions and by partial chemical analyses

which were used to calculate approximate structural formulas. Mg/Al ratios in the 9b octahedral site are either approximately equal to 2 or approximately equal to unity; alkali-site occupancy and ^{IV}Al decrease with increasing temperature and protons are generally deficient especially below 500°C. Tourmalines closely approaching the ideal defect end-member, $\square(Mg_2Al)Al_6(BO_3)_3Si_6O_{18}(OH)_4$, were synthesized at high temperatures.

When talc or mullite are present the substitution $Si^{4+} + Mg^{2+} = 2Al^{3+}$ predominates in the forward or reverse direction resulting in partial solid solution toward talc or mullite, respectively. Solid solution toward talc is also accompanied by the exchange of protons for small amounts of Mg^{2+}. The extent of substitution is approximately 25% toward mullite and 7.5% toward talc. Talc solid solutions containing as much as 3.6 mole% Al_2O_3 (Table 3) have also been synthesized. Subsolidus phase areas projected into the system MgO–Al_2O_3–SiO_2 include two, three-phase areas (tourmaline solid solution, quartz, talc or mullite) and one, two-phase area (tourmaline solid solutions, quartz).

Although the existence of tourmaline solid solutions in the system MgO–Al_2O_3–SiO_2–B_2O_3–H_2O has been demonstrated and the principal substitutions identified, the boundaries of the compositional field of tourmaline are not well defined at present. Furthermore, no information is available on the silica-deficient portion of the system. Single crystal studies of alkali-free tourmaline are necessary to determine the effect of the alkali-site vacancy on the structure and to account for the apparent preferred octahedral site occupancies and possible octahedral disordering. However, crystals large enough for such studies have not yet been synthesized.

Acknowledgments

The authors are indebted to the Departments of Metallurgy and Geology, Manchester University, England for use of the AEM and to Graham Cliff for technical assistance.

References

Champness, P. E., Cliff, G., and Lorimer, G. W. (1982) Quantitative analytical electron microscopy of metals and minerals. Ultramicroscopy, 8, 121–132.

Donnay, G. and Barton, R., Jr. (1972) Refinement of the crystal structure of elbaite and the mechanism of tourmaline solid solution. Tschermaks Mineralogische Petrographische Mitteilungen, 18, 273–286.

Dunn, P. J., Appleman, D. E., and Nelen, J. E. (1977a) Liddicoatite, a new calcium end-member of the tourmaline group. American Mineralogist, 62, 1121–1124.

Dunn, P. J., Appleman, D. E., Nelen, J. E., and Norberg, J. (1977b) Uvite, a new (old) common member of the tourmaline group and its implications for collectors. Mineralogical Record, 8, 100–108.

Foit, F. F., Jr. and Rosenberg, P. E. (1977) Coupled substitutions in the tourmaline group. Contributions to Mineralogy and Petrology, 62, 109–127.

Foit, F. F., Jr. and Rosenberg, P. E. (1979) The structure of vanadium-bearing tourmaline and its implications regarding tourmaline solid solutions. American Mineralogist, 64, 788–798.

Fortier, S. and Donnay, G. (1975) Schorl refinement showing composition dependence of the tourmaline structure. Canadian Mineralogist, 13, 173–177.

Kitahara, J. (1966) On dravite (Mg-tourmaline) from the Hirose mine, Tottori Prefecture. Journal Japanese Association of Mineralogists, Petrologists and Economic Geologists, 56, 228–233 (Japanese with English summary).

Ozaki, M. (1982) Mineralogical properties of the natural and synthetic aluminum-rich tourmalines. Ganseki Kobutsu Kosho Gakkaishi, 77, 375–386.

Rosenberg, P. E. and Foit, F. F., Jr. (1975) Alkali free tourmalines in the system MgO–Al_2O_3–SiO_2–B_2O_3–H_2O. (abstr.) Geological Society of America Abstracts with Programs, 7, 1250.

Rosenberg, P. E. and Foit, F. F., Jr. (1977) Crystal chemistry of alkali-free tourmaline. (abstr.) Geological Society of America Abstracts with Programs, 9, 1147–1148.

Rosenberg, P. E. and Foit, F. F., Jr. (1979) Synthesis and characterization of alkali-free tourmaline. American Mineralogist, 64, 180–186.

Swanson, H. E., Morris, M. C., Evans, E. H., and Verner, L. (1964) Standard X-ray diffraction patterns. National Bureau of Standards Monograph 25, Sec. 3, 47–48.

Towatana, P. (1985) Crystal chemistry of tourmalines from the Jack Creek dumortierite deposit, Basin, Montana. M.S. Thesis, Washington State University, Pullman.

Walsh, D., Donnay, G., and Donnay, J. D. H. (1974) Jahn-Teller effects in ferro-magnesian minerals: Pyroxenes and olivines. Bulletin of the Society of French Mineralogical Crystallography, 97, 170–183.

Werding, G. and Schreyer, W. (1984) Alkali-free tourmaline in the system MgO–Al_2O_3–SiO_2–B_2O_3–H_2O. Geochimica et Cosmochimica Acta, 48, 1331–1344.

Manuscript received, October 3, 1984;
accepted for publication, June 19, 1985.